STRUCTURAL SCIENCE
CRYSTAL ENGINEERING
MATERIALS

ISSN: 2052-5206
journals.iucr.org/b

Resolving the structure of $TiBe_{12}$

Matthew L Jackson, Patrick A Burr and Robin W Grimes

Acta Cryst. (2016). B**72**, 277–280

Acta Cryst B
STRUCTURAL SCIENCE
CRYSTAL ENGINEERING
MATERIALS

ISSN 2052-5206

Resolving the structure of $TiBe_{12}$

Matthew L Jackson,[a,b] Patrick A Burr[c]* and Robin W Grimes[a]

[a]Centre for Nuclear Engineering, Department of Materials, Imperial College, London SW7 2AZ, England, [b]Culham Centre for Fusion Energy, Culham Science Centre, Abingdon, Oxfordshire OX14 3DB, England, and [c]School of EEandT, University of New South Wales, Sydney, NSW 2052, Australia. *Correspondence e-mail: p.burr@unsw.edu.au

Received 8 December 2015
Accepted 25 February 2016

Edited by C. J. Howard, University of Newcastle, Australia

Keywords: beryllide; lattice dynamics; density functional theory; quasi-harmonic; thermal expansion.

CCDC reference: 1455788

Supporting information: this article has supporting information at journals.iucr.org/b

There has been considerable controversy regarding the structure of $TiBe_{12}$, which is variously reported as hexagonal and tetragonal. Lattice dynamics simulations based on density functional theory (DFT) show the tetragonal phase space group *I*4/*mmm* to be more stable over all temperatures, while the hexagonal phase exhibits an imaginary phonon mode, which, if followed, would lead to the cell adopting the tetragonal structure. We then report the predicted ground state elastic constants and temperature dependence of the bulk modulus and thermal expansion for the tetragonal phase.

1. Introduction

$TiBe_{12}$ is a promising candidate for neutron multiplier applications in future fusion reactors due to its exceptional combination of material properties (Dorn *et al.*, 2009). Based on earlier investigations (Raeuchle & Rundle, 1952; Raeuchle & von Batchelder, 1955; Zalkin *et al.*, 1961; Gillam *et al.*, 1964), several modern papers equally assume both hexagonal (Dorn *et al.*, 2009; Liu *et al.*, 2015; Peng, 2015) and tetragonal (Kurinskiy *et al.*, 2013; Munakata *et al.*, 2007; Reimann *et al.*, 2009; Chakin *et al.*, 2011) structures. In particular, most of the modelling efforts have been carried out on the hexagonal structure (Liu *et al.*, 2015; Peng, 2015). Both structures can be found in the crystallographic structure databases suggesting that they provide an equivalent description of the unit cell. However, simple nearest neighbor analysis shows that in fact they are distinct. Which structure corresponds to the reality is not *a priori* clear and requires special study. Here we review the discussion on the structure of $TiBe_{12}$ and, with the aid of density functional theory (DFT) and quasi-harmonic phonon calculations, investigate the relative stability of both structures.

The crystal structure of $TiBe_{12}$ was first identified by Raeuchle & Rundle (1952), from single-crystal measurements, as disordered hexagonal with lattice parameters a = 29.44 and c = 7.33 Å. In a later report concerned with the (tetragonal) structure of $MoBe_{12}$, Raeuchle & von Batchelder (1955) state that the structure of $TiBe_{12}$ was complex and 'in fact, is not yet completely known'. In the article they further discuss how their investigation into $MoBe_{12}$ provided clues that could refine the $TiBe_{12}$ structure previously reported, and 'that the refinement will increase the similarity between the two structures'. Subsequent publications by Zalkin *et al.* (1961) and then by Gillam *et al.* (1964), who used powder samples, reported a tetragonal structure analogous to $MoBe_{12}$ (prototype $Mn_{12}Th$) with lattice parameters a = 7.35 and c = 4.19 Å. This structure is also common among iso-stoichiometric transition metal beryllides (*e.g.* VBe_{12}, $CrBe_{12}$, $MoBe_{12}$,

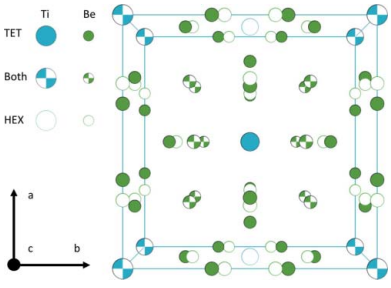

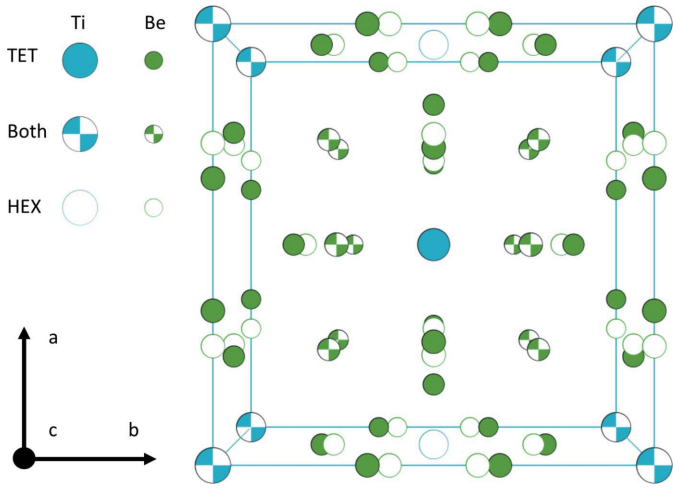

Figure 1
Correspondence between the *I*4/*mmm* tetragonal structure and the *P*6/*mmm* sub-cell for $TiBe_{12}$. In *I*4/*mmm* the *a* direction corresponds to the *c* direction in *P*6/*mmm*. Alternate Ti atoms are displaced by $\frac{1}{2}$ in the *I*4/*mmm* [100] direction/*P*6/*mmm* [0001] direction. Be positions are only slightly perturbed.

WBe_{12}; von Batchelder & Raeuchle, 1957). Furthermore, Gillam *et al.* (1964) provided the structural relationship between $TiBe_{12}$ and Ti_2Be_{17}, which led to their conclusion that 'Raeuchle and Rundle's [hexagonal] structure determination was carried out on crystals of Ti_2Be_{17} instead of crystals of $TiBe_{12}$' (Gillam *et al.*, 1964). In fact, the two $TiBe_{12}$ phases are also closely related (Fig. 1), and produce similar diffraction patterns as demonstrated in Fig. 2.

Several recent studies (Liu *et al.*, 2015; Peng, 2015) have used/assumed a sub-cell of the hexagonal crystal structure identified by Raeuchle & Rundle (1952) with lattice parameters of a = 4.26 and c = 7.33 Å. This differs from the structure defined by the full unit cell in that Ti atoms between alternate sub-cells should be displaced by $\pm\frac{1}{2}$[0001] in a disordered fashion. As such, this sub-cell is not a true representation of the crystal structure reported by Raeuchle & Rundle (1952)

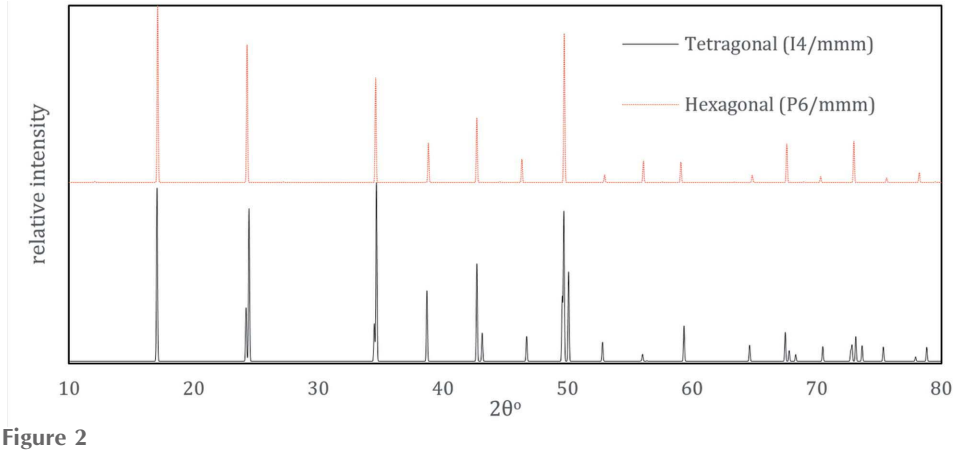

Figure 2
Simulated diffraction patterns for the fully ordered *P*6/*mmm* and *I*4/*mmm* unit cells.

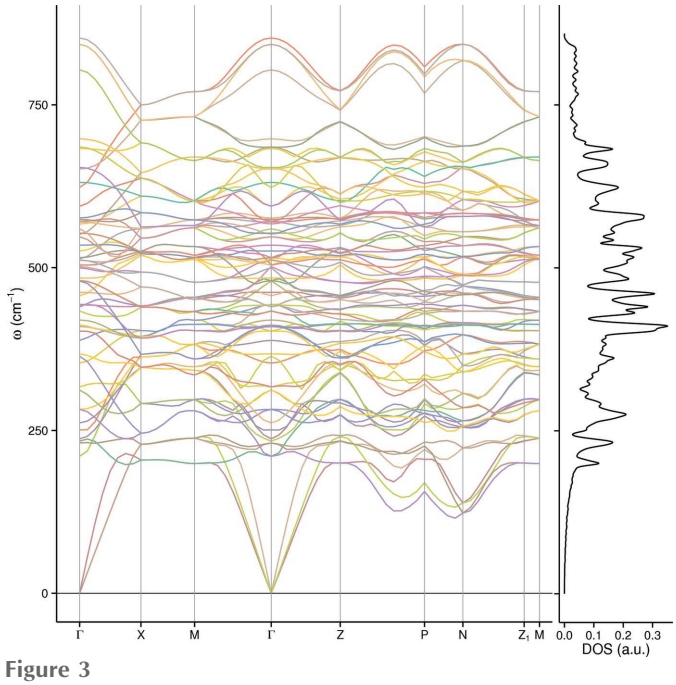

Figure 3
Dispersion curve and DOS of the tetragonal *I*4/*mmm* $TiBe_{12}$ structure.

2. Density functional theory simulations

Both the tetragonal structure and the hexagonal sub-cell were modelled with the *Castep* (Clark *et al.*, 2005) DFT code using plane waves with an energy cut-off of 480 eV and ultrasoft pseudopotentials; k-points spacing was kept below 0.3 nm^{-1}. The structures were relaxed until atomic forces and stresses were less than 10^{-3} eV $Å^{-1}$ and 10^{-2} eV $Å^{-2}$, respectively.

First the classical ground state of the systems was calculated following equation (1)

$$E_f(TiBe_{12}) = E^{DFT}(TiBe_{12}) - E^{DFT}(Ti) - 12E^{DFT}(Be). \quad (1)$$

The formation energies of the hexagonal and tetragonal phases were found to be −6.82 and −7.90 eV per formula unit, respectively. A difference in formation energy as large as 1.08 eV suggests that the tetragonal phase is stable at low temperatures. However, zero point energy and temperature effects also contribute to relative stability; these are considered next.

The phonon dispersion curves and density of states (DOS) were computed using the supercell method to evaluate the dynamical matrix from the force constant matrix (Parlinski *et al.*, 1997). Supercells containing 54 and 234 atoms were used for the tetragonal structure and supercells containing 54 and 312 atoms were used for the hexagonal sub-cell. The resulting dispersion curves from the larger supercells are presented in Figs. 3

Table 1
Lattice parameters and elastic constants of tetragonal $TiBe_{12}$.

Hill's (1952) average was used to calculate ground state shear (G) and bulk (K) moduli.

	a (Å)	c (Å)	c_{11} (GPa)	c_{12} (GPa)	c_{13} (GPa)	c_{33} (GPa)	c_{44} (GPa)	c_{66} (GPa)	K (GPa)	G (GPa)
DFT ground state	7.359	4.164	362.4	2.4	20.8	327.5	129.6	117.2	126.7	140.8
DFT QH (T = 0 K)	7.446	4.216	–	–	–	–	–	–	123.6	–
DFT QH (T = 300 K)	7.457	4.223	–	–	–	–	–	–	121.4	–
Experimental (T = 273 K)	7.35[a]	4.19[a]	–	–	–	–	–	–	117.0[b]	–

References: (*a*) Zalkin *et al.* (1961); (*b*) Fleischer & Zabala (1989).

and 4. It is evident that the hexagonal structure contains a soft mode at the M-point – a clear indication of instability in the ground state. Following this mode would lead to a hexagonal/tetragonal transformation as it displaces Ti and a Be in ⟨0001⟩ directions to their corresponding positions in the tetragonal phase.

Zero-point energy and temperature contributions to the Helmholtz free energy were obtained by integrating the phonon DOS, following the harmonic and quasi-harmonic approximations, as outlined in Burr *et al.* (2015). Fig. 5 shows the combined internal (U) and Helmholtz (F) free energy for both systems as a function of temperature up to 1800 K. The excellent agreement between the small supercell and large supercell calculations provide confidence that the 54-atom supercells are adequate for phonon calculations in these systems. Consequently, the quasi-harmonic method was carried out with the 54-atom supercells only. It is evident that the tetragonal *I*4/*mmm* structure is consistently more stable compared with hexagonal *P*6/*mmm*, in line with the thermodynamic instability of the hexagonal structure.

3. Properties of *I*4/*mmm* $TiBe_{12}$

Now that the structure of $TiBe_{12}$ is established, we report some of its fundamental material properties that arise from the quasi-harmonic approach (see the supporting information for calculation details). These are presented in Fig. 6 and Table 1, together with experimental data where available.

The thermal expansion of the tetragonal phase compares favourably to the available experimental data. The bulk modulus follows a typical relationship with temperature for a metal, decreasing with increasing temperature. Predicted lattice constants are slightly overestimated when thermal effects are taken into account, however the bulk modulus is extremely close to the experimental value. This is the first report of stiffness constants for *I*4/*mmm* $TiBe_{12}$.

4. Conclusion

Using atomic scale quantum mechanical simulations we have investigated the controversy regarding the crystal structure of

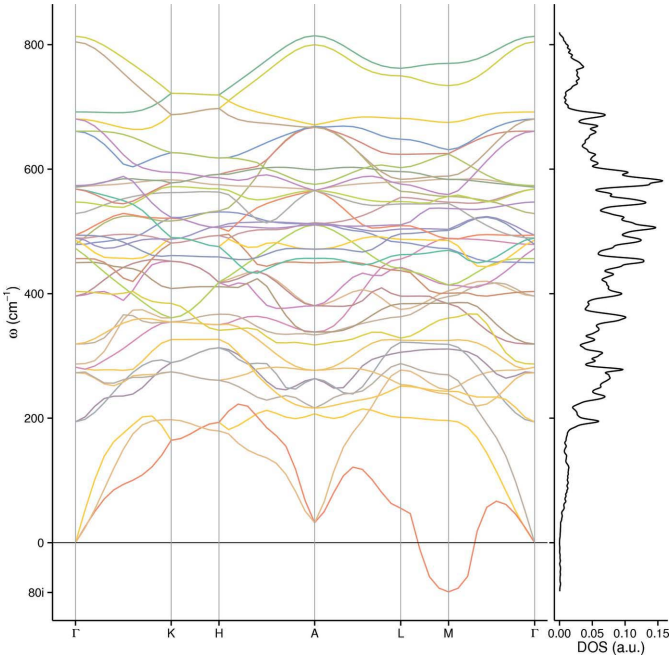

Figure 4
Dispersion curve and DOS for the hexagonal *P*6/*mmm* sub-cell of $Ti_{12}Be$.

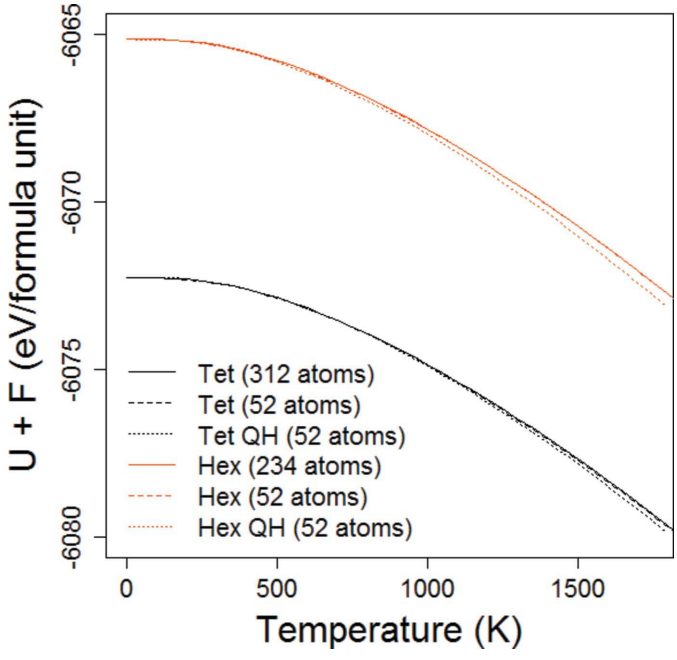

Figure 5
Internal + free energy as a function of temperature. QH = quasi-harmonic. Harmonic results with different supercell sizes appear so close as to be indistinguishable.

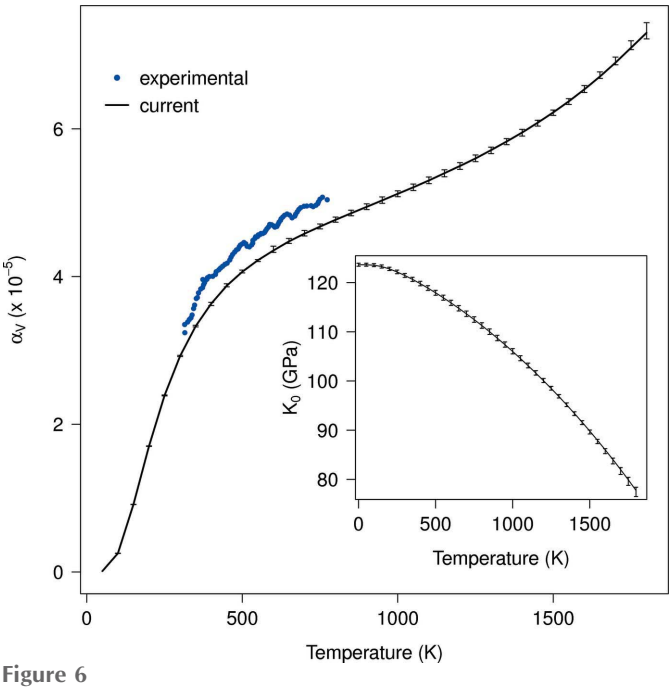

Figure 6
Volumetric thermal expansion coefficient (α_V) and bulk modulus (K_0) of tetragonal $TiBe_{12}$ (Reimann *et al.*, 2009).

$TiBe_{12}$, originating from papers published between 1952 and 1964. Lattice dynamics simulations for $TiBe_{12}$ are consistent with the tetragonal structure proposed by Zalkin *et al.* (1961) and by Gillam *et al.* (1964; space group *I*4/*mmm*), not the hexagonal structure proposed by Raeuchle & Rundle (1952; space group *P6/mmm*), or the derivative hexagonal sub-cell that has been used recently in modelling studies (Liu *et al.*, 2015; Peng, 2015). While larger supercells are investigated, the 54 atom cell was sufficient to calculate the phonon density of states. Further, for this system little difference was found between harmonic and quasi-harmonic based contributions to the Helmzoltz free energy. Elastic and thermal expansion data for the tetragonal phase are also reported, which are useful for further consideration of the material as a structural component in fusion reactor applications.

5. Related literature

The following references are cited in the supporting information: Birch (1978) and Murnaghan (1944)

Acknowledgements

MLJ thanks CCFE and PAB thanks the EPSRC and ANSTO for financial support. The computing resources were provided by Imperial College HPC.

References

Batchelder, F. W. von & Raeuchle, R. F. (1957). *Acta Cryst.* **10**, 648–649.
Birch, F. (1978). *J. Geophys. Res.* **83**, 1257–1268.
Burr, P. A., Middleburgh, S. C. & Grimes, R. W. (2015). *J. Alloys Compd.* **639**, 111–122.
Chakin, V., Klimenkov, M., Rolli, R., Kurinskiy, P., Moeslang, A. & Dorn, C. (2011). *J. Nucl. Mater.* **417**, 769–774.
Clark, S. J., Segall, M. D., Pickard, C. J., Hasnip, P. J., Probert, M. I. J., Refson, K. & Payne, M. C. (2005). *Z. Kristallogr.* **220**, 567–570.
Dorn, C. K., Haws, W. J. & Vidal, E. E. (2009). *Fusion Eng. Des.* **84**, 319–322.
Fleischer, R. L. & Zabala, R. J. (1989). *Metall. Trans. A*, **20**, 1279–1282.
Gillam, E., Rooksby, H. P. & Brownlee, L. D. (1964). *Acta Cryst.* **17**, 762–763.
Hill, R. (1952). *Proc. Phys. Soc. A*, **65**, 349–354.
Kurinskiy, P., Moeslang, A., Chakin, V., Klimenkov, M., Rolli, R., van Til, S. & Goraieb, A. A. (2013). *Fusion Eng. Des.* **88**, 2198–2201.
Liu, X. K., Zhou, W., Liu, X. & Peng, S. M. (2015). *RSC Adv.* **5**, 59648–59654.
Munakata, K., Kawamura, H. & Uchida, M. (2007). *J. Nucl. Mater.* **367–370**, 1057–1062.
Murnaghan, F. D. (1944). *Proc. Natl. Acad. Sci. USA*, **30**, 244–247.
Parlinski, K., Li, Z. Q. & Kawazoe, Y. (1997). *Phys. Rev. Lett.* **78**, 4063–4066.
Peng, S. M. (2015). *J. Nucl. Mater.* **464**, 230–235.
Raeuchle, R. F. & Rundle, R. E. (1952). *Acta Cryst.* **5**, 85–93.
Raeuchle, R. F. & von Batchelder, F. W. (1955). *Acta Cryst.* **8**, 691–694.
Reimann, J., Kurinskiy, P., Lindau, R., Moeslang, A., Rohde, M., Dorn, C., Haws, W., Goraieb, A., Harsch, H. & Linsmeier, C. (2009). 23rd IEEE/NPSS Symposium of Fusion Engineering.
Zalkin, A., Sands, D. E., Bedford, R. G. & Krikorian, O. H. (1961). *Acta Cryst.* **14**, 63–65.